SUPPLEMENTARY FIGURES

Host-Pathogen Pyrimidine Metabolism Drives Cystic Fibrosis Lung Disease

Gaurav Kumar Lohia[1], Ying-Tsun Chen[1], Samantha Chen[1], Ayesha Beg[1], Erin Theiller[2], Aomeng Cui[3,4], Ahmed M Moustafa[2], Sebastián A. Riquelme[1,*]

[1]Department of Pediatrics, Division of Infectious Diseases, Columbia University Medical Center, New York, NY, USA.

[2]Division of Gastroenterology, Hepatology, and Nutrition, The Children's Hospital of Philadelphia, Philadelphia, PA 19104, USA; Department of Pediatrics, Perelman School of Medicine, University of Pennsylvania, Philadelphia, PA 19104, USA; Center for Microbial Medicine, Children's Hospital of Philadelphia, Philadelphia, PA, USA.

[3]Vagelos College of Physicians and Surgeons, Columbia University Irving Medical Center, New York, NY USA

[4]Department of Neurology, Columbia University Irving Medical Center, New York, NY USA

* Corresponding author: sr3302@cumc.columbia.edu

Supplementary Figure 1

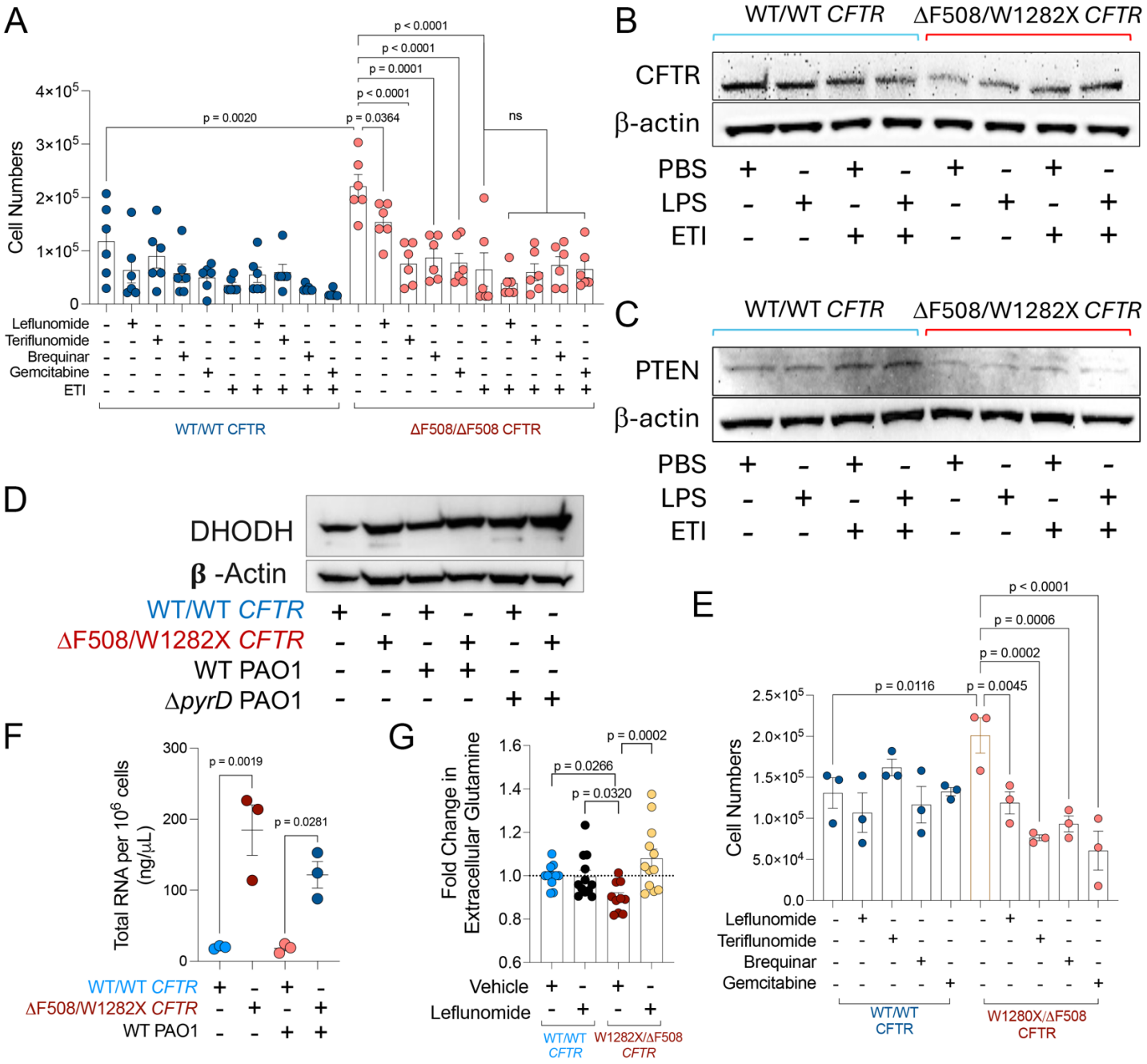

Supplementary Figure 1. CFTR dysfunction drives pyrimidine metabolic reprogramming and pathological airway cell growth — A) Number of CF (ΔF508/ΔF508 CFTR) and non-CF (WT/WT CFTR) primary bronchial epithelial cells exposed for 48h to different DHODH inhibitors (leflunomide, teriflunomide, brequinar) or the pyrimidine analog, chemotherapeutical agent gemcitabine (N=3, including all replicates). WT/WT and ΔF508/W1282X CFTR cells were exposed to either PBS, LPS, ETI, WT PAO1, Δ*pyrD* PAO1, or the different DHODH inhibitors (N=3). Then, 24h later the following were measured: **B**) CFTR expression; **C**) PTEN levels; **D**) DHODH expression; **E**) cell numbers; **F**) Total RNA abundance; **G**) extracellular glutamine. Data: mean ± SEM across *N* = 3 independent experiments, with a total of the following number of biological replicates (*n*): A, *n* = 6 ; F, E, *n* = 3; G, n = 12 (WT/WT CFTR ± leflunomide, ΔF508/W1282X CFTR + leflunomide), *n* = 10 (ΔF508/W1282X CFTR + Vehicle). Stats — A, G, E: One-Way ANOVA (mixed model, Tukey *post-hoc* test); F: t-Student (two-tailed, Welch's test). ****: $P < 0.0001$; ***: $P < 0.001$; **: $P < 0.01$; *: $P < 0.05$; ns: non-significant.

Supplementary Figure 2

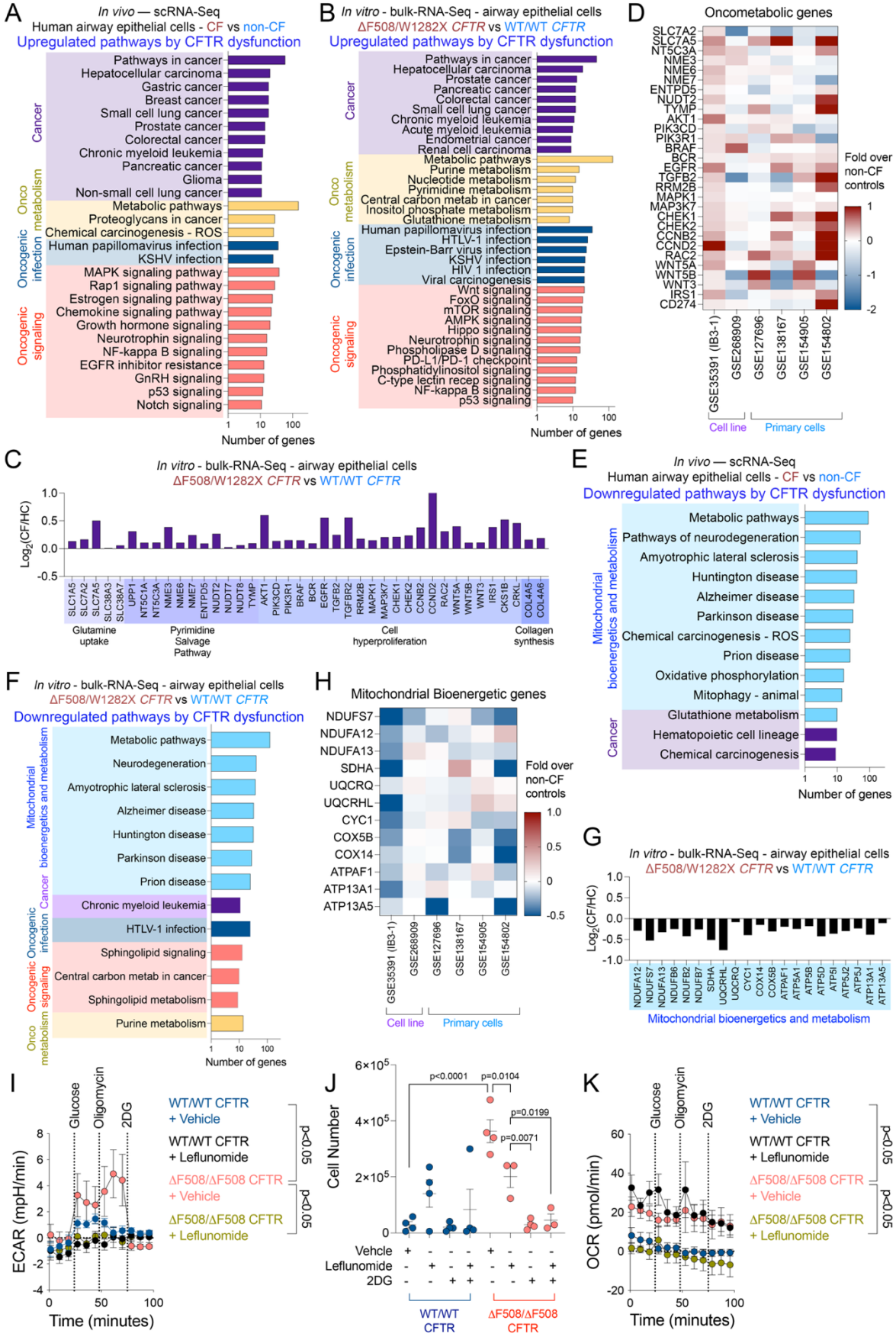

Supplementary Figure 2. CFTR mutations promote mitochondrial changes consistent with oncometabolic-like reprogramming — A) scRNA-seq and pathway enrichment analysis of significantly (P<0.05) increased genes in non-CF and CF airway epithelial cells from the human lung. In WT/WT and ΔF508/W1282X CFTR airway epithelial cells the following was analyzed via bulk-RNA-Seq: **B**) Pathway enrichment analysis of all increased genes via bulk-RNA-seq; **C**) Significantly (P<0.05) upregulated genes; **D**) oncometabolic genes in this and many other data sets (GEO accession numbers in labels). **E**) scRNA-seq and pathway enrichment analysis of significantly (P<0.05) decreased transcripts in non-CF and CF airway epithelial cells from the human lung. In WT/WT and ΔF508/W1282X CFTR airway epithelial cells the following was analyzed via bulk-RNA-Seq: **F**) Pathway enrichment analysis of all reduced genes via bulk-RNA-seq; **G**) Significantly (P<0.05) downregulated genes **H**) mitochondrial bioenergetic genes in this and many other data sets (GEO accession numbers in labels). WT/WT and ΔF508/ΔF508 CFTR primary bronchial epithelial cells were seeded (~$5x10^4$/well) and, when indicated, exposed to either vehicle, leflunomide, uridine or 2DG. The following were measured: **I**, **K**) At 4h, ECAR and oxygen consumption rate (OCR); **J**) at 48h, cell growth. Data: mean ± SEM across *N* = 3 independent experiments, with a total of the following number of biological replicates (*n*): I and K, *n* = 10 (WT/WT CFTR and ΔF508/ΔF508 CFTR), *n* = 5 (WT/WT CFTR + leflunomide and ΔF508/ΔF508 CFTR + leflunomide); J, *n* = 4 (WT/WT CFTR: Vehicle, leflunomide, 2-DG, leflunomide + 2-DG; ΔF508/ΔF508 CFTR: Vehicle, 2-DG), *n* = 3 (ΔF508/ΔF508 CFTR: leflunomide, leflunomide + 2-DG). Stats — A-G: *P*-values were adjusted for multiple comparisons (FDR-corrected). J: One-Way ANOVA (mixed model, Tukey *post-hoc* test); I, K: repeated measures ANOVA on ranks (Dunn's multiple comparison test). ****: $P < 0.0001$; ***: $P < 0.001$; **: $P < 0.01$; *: $P < 0.05$; ns: non-significant.

Supplementary Figure 3

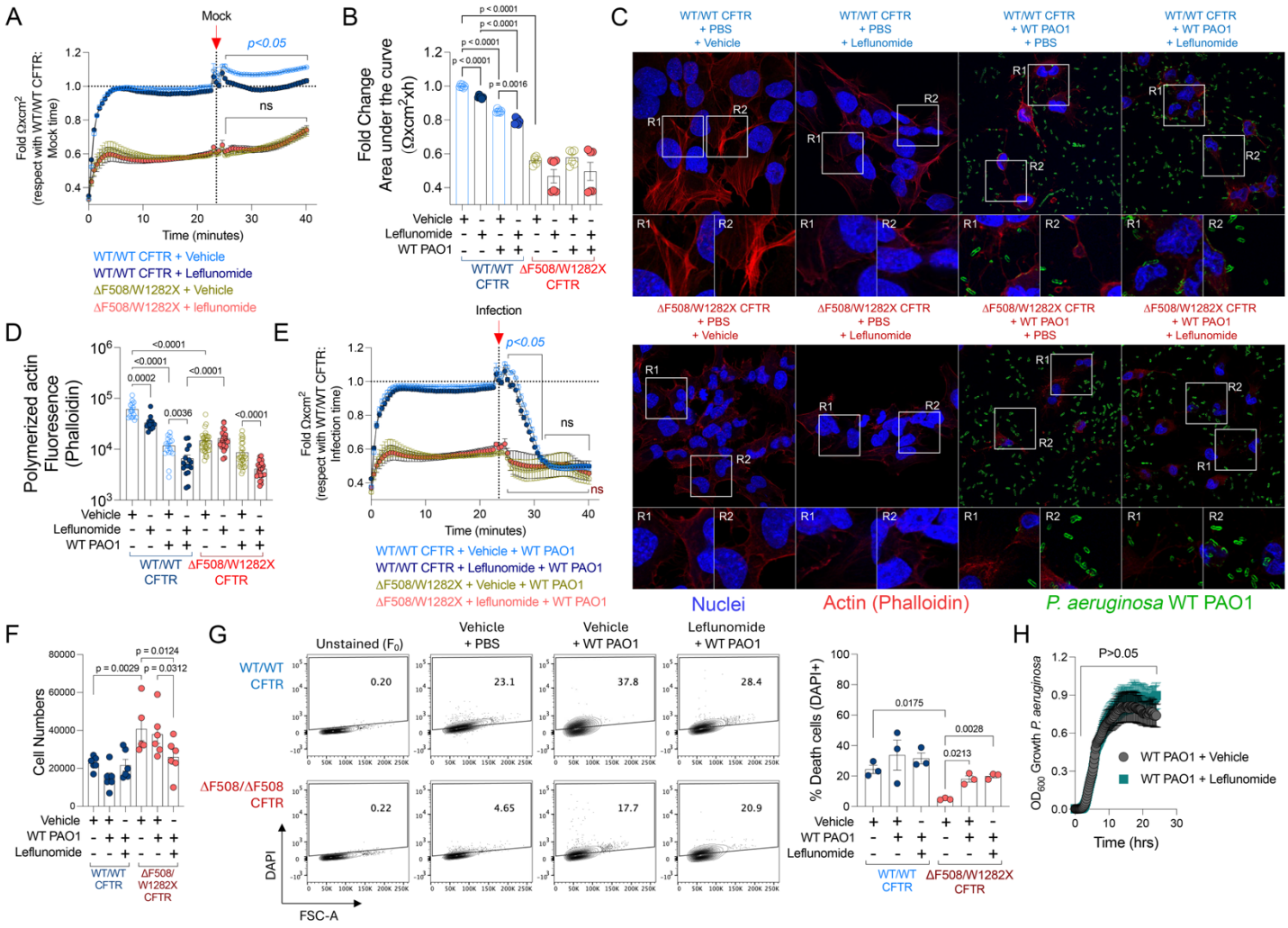

Supplementary Figure 3. DHODH does not influence CF airway cell barrier dysfunction — WT/WT and ΔF508/W1282X CFTR cells were exposed to leflunomide, vehicle, and PBS or *P. aeruginosa* WT PAO1 (N=2). Then, the following were analyzed: **A**, **E**) transepithelial electrical resistance (TEER) (total of 40h including infection/mock (PBS); **B**) total resistance (area under the curve in A and E); **C**) total actin polymerization after 6h (phalloidin staining). Bacteria marked with an anti-*P. aeruginosa* antibody and shown in green; **D**) quantification of total polymerized actin at 6h; **F**) total cell numbers (24h); **G**) left — flow cytometry contour plots gating dead (DAPI+) cells/right — quantification of % of $DAPI^+$ gated cells. **H**) WT PAO1 growth in the presence or not of leflunomide. Data: mean ± SEM across *N* = 3 independent experiments, with a total of the following number of biological replicates (*n*): A-B, E, *n* = 6; D, *n* (number of images/number of cells studied) : WT/WT CFTR: 3/16 (PBS), 3/15 (leflunomide), 3/17 (WT PAO1), 3/17 (WT PAO1 + leflunomide), ΔF508/W1282X CFTR: 3/36 (PBS), 3/23 (leflunomide), 3/31 (WT PAO1), 3/25 (WT PAO1+leflunomide); F, *n* = 6 (WT/WT CFTR: Vehicle, leflunomide, WT PAO1+ leflunomide, ΔF508/W1282X CFTR: WT PAO1, WT PAO1+leflunomide), 5 (ΔF508/W1282X CFTR Vehicle); G, *n* = 3; H, *n* = 11. Stats — B, D, F, G: One-Way ANOVA (mixed model, Tukey *post-hoc* test); A, E, H: repeated measures ANOVA on ranks (Dunn's multiple comparison test). ****: $P < 0.0001$; ***: $P < 0.001$; **: $P < 0.01$; *: $P < 0.05$; ns: non-significant.

Supplementary Figure 4

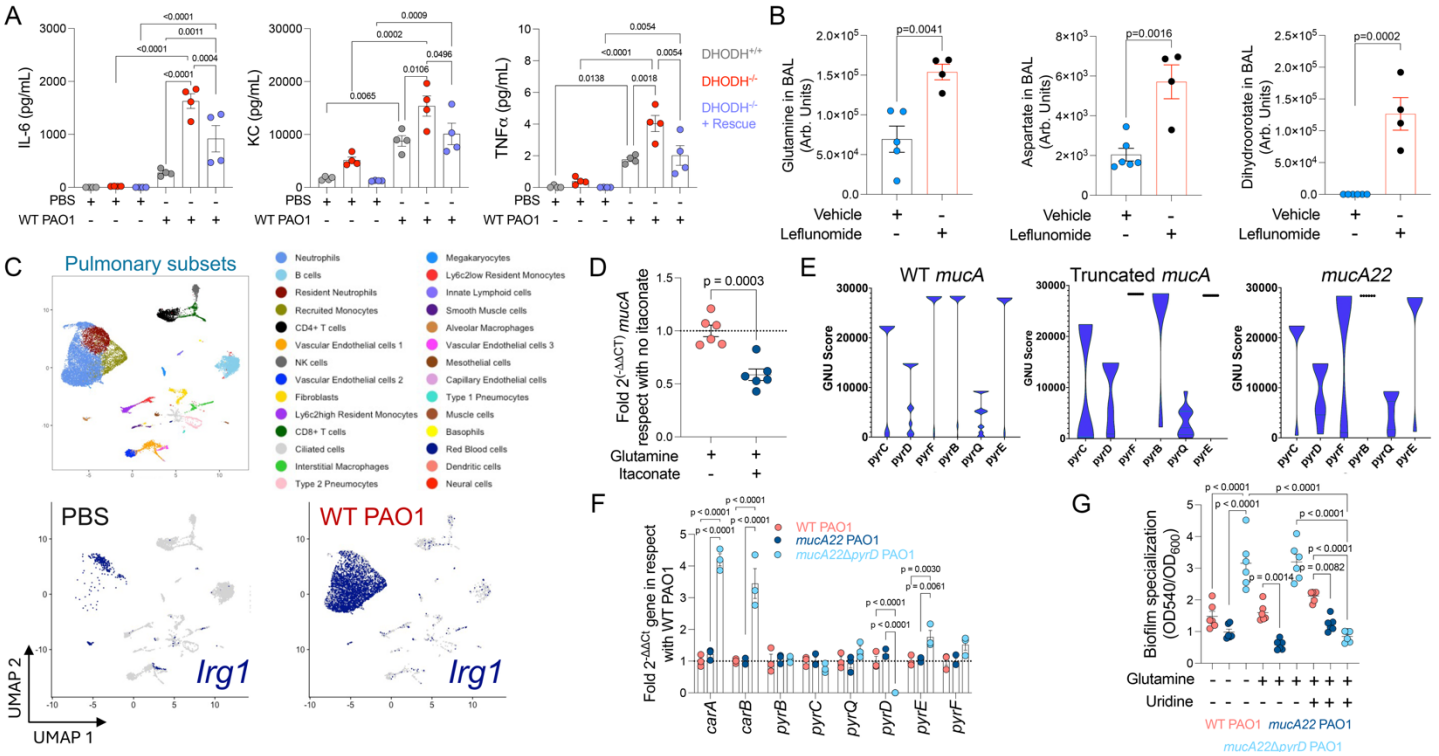

Supplementary Figure 4. Modulation of cytokine release and *P. aeruginosa* adaptation by the DHODH-itaconate axis — A) Pro-inflammatory cytokines released by control, DHODH$^{-/-}$, and DHODH$^{-/-}$ rescued 4T1 carcinoma cells during 24h WT PAO1 infection (N=3). **B**) Airway metabolite levels after 24h administration of leflunomide to mice (N=3). **C**) *Irg1* expression in different lung cell populations via scRNA-Seq (24h post infection). **D**) *mucA* fold mRNA expression in WT PAO1 exposed or not to itaconate for 24h. **E**) DNPPS cluster conservation frequency in *P. aeruginosa* isolates harboring different *mucA* alterations. **F**) mRNA levels of different genes involved in bacterial DNPPS (N=3). **G**) Bacteria biofilm community specialization (OD_{590}/OD_{600}) (N=3). Data: mean ± SEM across *N* = 3 independent experiments, with a total of the following number of biological replicates (*n*): A, *n* = 4; B, Vehicle: *n* = 5 (Glutamine), 6 (Aspartate and DHO); Leflunomide: *n* = 4; D, *n* = 6; F, *n* = 3; G, *n* = 6. N = 3 independent experiments. Stats — A, F-G: One-Way ANOVA (mixed model, Tukey *post-hoc* test); B, D: t-Student (two-tailed, Welch's test); C: *P* values were adjusted for multiple comparisons (FDR-corrected). ****: $P < 0.0001$; ***: $P < 0.001$; **: $P < 0.01$; *: $P < 0.05$; ns: non-significant.

Supplementary Figure 5

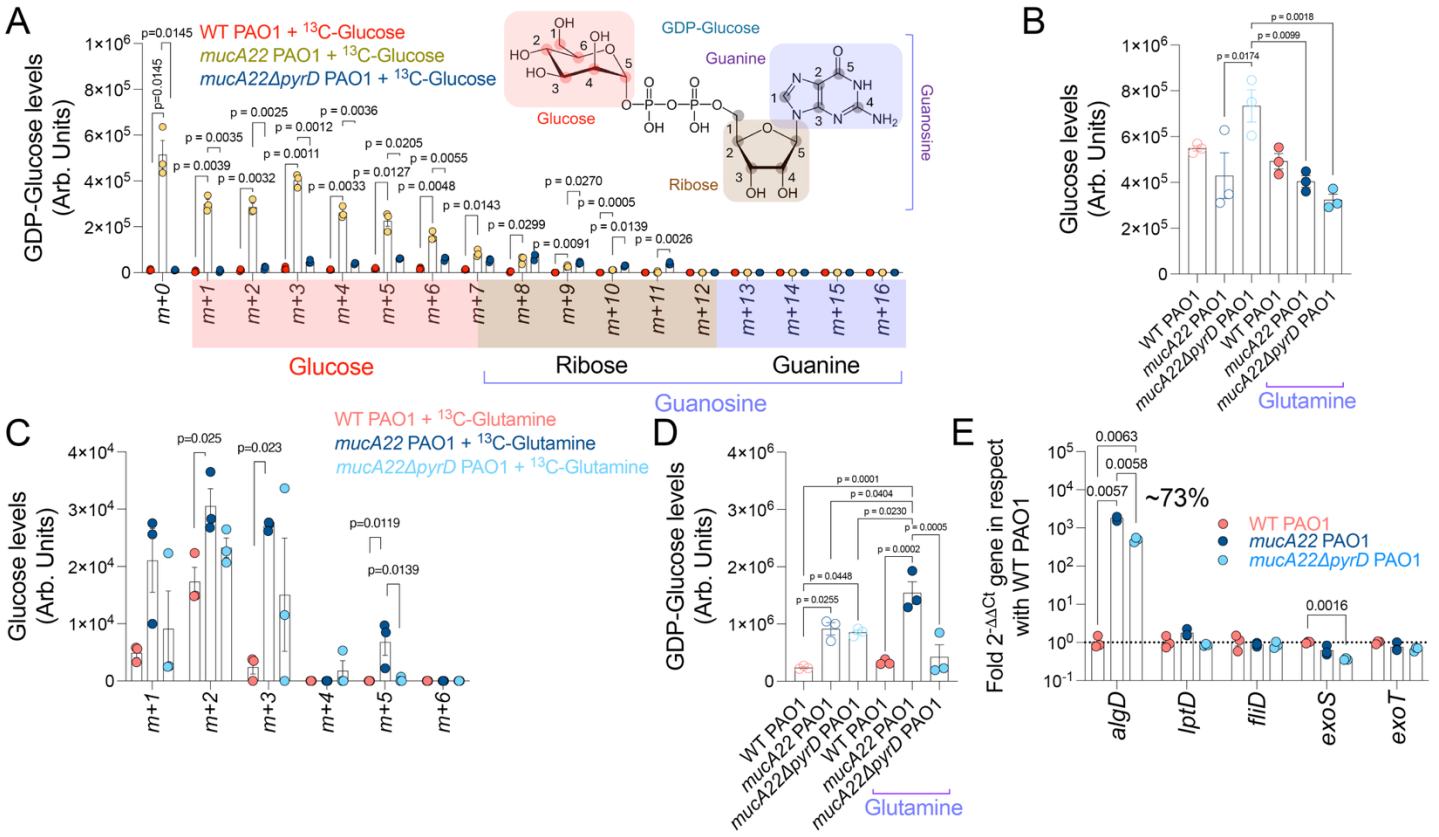

Supplementary Figure 5. *PyrD* shapes metabolic fitness in *mucA*-deficient *P. aeruginosa* strains — WT PAO1, *mucA22* PAO1, and *mucA22ΔpyrD* PAO1 were exposed or not to either ^{13}[C]-glucose or ^{13}[C]-glutamine for 6h. Then, the following was measured (N=3): **A)** GDP-glucose isotopomers (*m+1*, *m+16*) (carbon tracing); **B**) total glucose; **C**) glucose isotopomers (carbon tracing); **B**) total GDP-glucose. **E**) Gene expression (N=3). Data: mean ± SEM across *N* = 3 independent experiments, with a total of the following number of biological replicates (*n*): A-E, *n* = 3. Stats — A-E One-Way ANOVA (mixed model, Tukey *post-hoc* test). ****: $P < 0.0001$; ***: $P < 0.001$; **: $P < 0.01$; *: $P < 0.05$; ns: non-significant.

Supplementary Figure 6

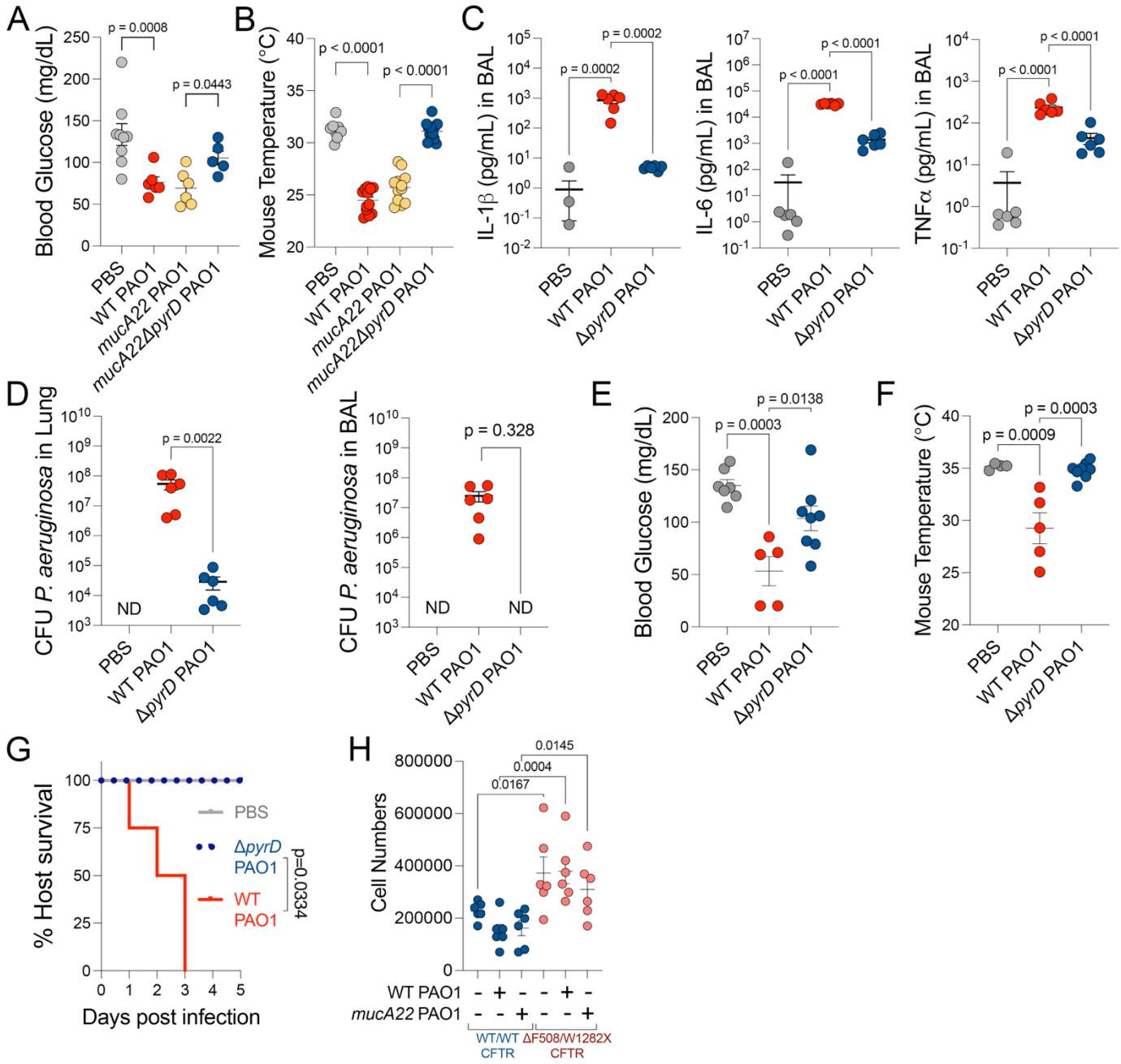

Supplementary Figure 6. *PyrD* promotes systemic *P. aeruginosa* disease — Mice were exposed to either PBS, WT PAO1, *mucA22* PAO1, or *mucA22*Δ*pyrD* PAO1 (N=3, 5-12 mice in total). Then, 24h later the following were measured: **A**) glycemia; **B**) core body temperature. **C**) survival. Animals were exposed to either PBS, WT PAO1, or a Δ*pyrD* PAO1 strain (N=3, 5-8 mice in total). The following were measured: **C**) BAL cytokines; **D**) lung/BAL CFUs; **E**) glycemia; **F**) core body temperature; **G**) survival. **H**) Number of WT/WT and ΔF508/W1282X CFTR airway epithelial cells exposed for 24h to either PBS, WT PAO1, or *mucA22* PAO1 (N=3, including replicates). Data: mean ± SEM across *N* = 3 independent experiments, with a total of the following number of biological replicates (*n*): A, *n* = 9 (PBS), 6 (WT PAO1, *mucA22* PAO1), 5 (*mucA22*Δ*pyrD* PAO1); B, *n* = 8 (PBS), 12 (WT PAO1, *mucA22* PAO1, *mucA22*Δ*pyrD* PAO1); C, *n* = 6; D, *n* = 3 (PBS), 6 (Δ*pyrD* PAO1); E, *n* = 7 (PBS), 5 (WT PAO1) , 8 (Δ*pyrD* PAO1); F, *n* = 4 (PBS) , 5 (WT PAO1), 8 (Δ*pyrD* PAO1); H, *n* = 6. Stats — A-F, H: One-Way ANOVA (mixed model, Tukey *post-hoc* test); G: Kaplan-Meier. ****: $P < 0.0001$; ***: $P < 0.001$; **: $P < 0.01$; *: $P < 0.05$; ns: non-significant.

Supplementary Data 1: scRNA-seq Pathway Analysis of CF Airway Epithelial Cells from Human Lung Tissue. Publicly available scRNA-Seq datasets from human lung tissue were analyzed to identify differentially expressed genes using predefined statistical significance ($P < 0.05$) and fold-change thresholds. *P* values were adjusted for multiple comparisons using false discovery rate (FDR) correction. Genes meeting these criteria were subjected to pathway enrichment analysis using DAVID with KEGG pathway annotations, focusing on routes involved in pyrimidine metabolism, cell proliferation, fibrosis and mitochondrial function. Statistical significance of pathway enrichment was assessed using DAVID's modified Fisher's exact test (EASE score), with *P* values adjusted for multiple comparisons using the Benjamini–Hochberg false discovery rate (FDR) procedure.

Supplementary Data 2: Bulk-RNA-seq Pathway enrichment analysis of CF epithelial cell lines. Publicly available bulk RNA-seq datasets obtained from primary cells and cell lines grown *ex vivo* were analyzed to identify differentially expressed genes using predefined statistical significance ($P < 0.05$) and fold-change thresholds. *P* values were adjusted for multiple hypothesis testing using false discovery rate (FDR) correction. Pathway enrichment analysis was performed using DAVID with KEGG pathway annotations, putting special emphasis on those related to pyrimidine metabolism, cell proliferation, fibrotic signaling and mitochondrial function. Statistical significance of pathway enrichment was assessed using DAVID's modified Fisher's exact test (EASE score), with *P* values adjusted for multiple comparisons using the Benjamini–Hochberg false discovery rate (FDR) procedure.

Supplementary Data 3: NCBI entry numbers of *P. aeruginosa* genomes used for genetic analyses on pyrimidine metabolism.

Supplementary Data 4: Primers used in the study.